

# Bursting bubbles : a numerical convergence study

A. Berny<sup>a</sup>, L. Deike<sup>b</sup>, T. Seon<sup>c</sup> S. Popinet<sup>d</sup>

a. Sorbonne Universités, Sorbonne Université and Centre National de la Recherche Scientifique, Unité Mixte de Recherche 7190, Institut Jean Le Rond d'Alembert 4 Place Jussieu, F75005 Paris, France, berny[at]dalembert.upmc.fr

b. Department of Mechanical and Aerospace Engineering, Princeton University, Princeton, New Jersey 08544 USA

Princeton Environmental Institute, Princeton University, Princeton, New Jersey 08544, USA  
ldeike[at]princeton.edu

c. Sorbonne Universités, Sorbonne Université and Centre National de la Recherche Scientifique, Unité Mixte de Recherche 7190, Institut Jean Le Rond d'Alembert 4 Place Jussieu, F75005 Paris, France, thomas.seon[at]gmail.com

d. Sorbonne Universités, Sorbonne Université and Centre National de la Recherche Scientifique, Unité Mixte de Recherche 7190, Institut Jean Le Rond d'Alembert 4 Place Jussieu, F75005 Paris, France, popinet[at]basilisk.fr

## Résumé :

*L'éclatement de bulle est un phénomène omniprésent, allant des bulles dans un verre de champagne à la surface de l'océan ou l'éclatement de bulle est une source d'embruns. Nous réalisons ici des simulations numériques directes en 2D axi symétrique de l'éclatement d'une bulle au moyen du code de calcul en Volume Fini basilisk. Nous présentons une étude numérique de convergence de l'éclatement d'une bulle, dans des conditions air-eau pour les rapports de densité et de viscosité, pour une bulle particulière correspondant à un nombre de Laplace  $La = \rho_{liq}\gamma R_b / \mu_{liq}^2 = 20000$  et un nombre de Bond  $Bo = \rho_{liq}gR_b^2 / \gamma = 0.1$  ou  $\rho_{liq}$ ,  $\mu_{liq}$ ,  $\gamma$ ,  $R_b$  et  $g$  sont respectivement la masse volumique du liquide, la viscosité du liquide, la tension à l'interface, le rayon initial de la bulle et l'action de la gravité. Nous vérifions la convergence numérique en fonction de la taille de la grille, pour la vitesse du jet et la taille de la première goutte puis nous discutons la variabilité de nos résultats sur les gouttes qui suivent avec l'augmentation de la taille de la grille.*

## Abstract :

*Bursting bubbles is an ubiquitous phenomenon, from bubbles in a champagne glass, to the surface of the ocean, where bubbles burst and generate sea spray. Here we perform 2D axi-symmetric direct numerical simulations of the bursting of a single bubble with the basilisk Volume Of Fluid (VOF) solver. We present a numerical convergence study of a bubble bursting, with air-water density and viscosity ratio, for a particular case, corresponding to a Laplace number,  $La = \rho_{liq}\gamma R_b / \mu_{liq}^2 = 20000$ , and Bond number  $Bo = \rho_{liq}gR_b^2 / \gamma = 0.1$  where  $\rho_{liq}$ ,  $\mu_{liq}$ ,  $\gamma$ ,  $R_b$  and  $g$  are the liquid density, viscosity, interfacial tension, the initial bubble radius and the gravity action respectively. We verify numerical convergence*

with respect to grid size regarding the jet velocity, and the first droplet radius, and discuss the variability in the subsequent droplets for the increasing grid size.

**Mots clefs :** bubbles, drops, bursting, jet, ocean, numerical simulation

## 1 Introduction

When an air bubble reaches the liquid surface, the thin film forming the cap of the bubble drains and eventually ruptures [1]. The bursting of the film might produce tiny film droplets [2]. This leaves an unstable open cavity, which collapses due to capillary forces [3, 4]. This produces a central jet that arises and eventually breaks up, leading to 1 to 10 droplets [5, 6]. This mechanism occurs in many practical applications, from bubbles in a glass of sparkling wine which produce aerosols that spread in the air [7, 8] to bubbles at the surface of the ocean, produced by breaking waves [1]. Since the first study of this phenomenon by Woodcock *et al.* in 1953 [9], numerous studies have described the bursting bubbles phenomenon. In 2002 Duchemin *et al.* [3] performed the first direct numerical simulation of a bursting bubble with a free surface Navier-Stokes equation formulation. They characterized the size and the velocity of the first drop neglecting the effect of gravity. More recently, Ghabache *et al.* experimentally characterized the velocity [4] and the size [6] of the first drop. Deike *et al.* [10] performed numerical simulations that fully describe the velocity of the first drop for a large range of parameters. At the same time, Brasz *et al.* by the use of experiments and numerical simulations [11] characterized the size of the first drop. Ganan-Calvo proposed a scaling law to describe the size and the velocity of the first drop [12, 13] in good agreement with experiments and numerical simulations while Gordillo and Rodriguez-Rodriguez [14] proposed an alternative model that describes the velocity of the first drop. This body of works provides a precise description of the size and velocity of the first drop. Earlier studies by Spiel [5] provided a first study on the number of ejected droplets and the statistics of the size of the subsequent droplet in air-water conditions. However, the precise knowledge of the number, size, and velocity of all droplets for a wide range of parameters remains to be clarified. Here we develop direct numerical simulations that capture all the jet drops produced by a bursting bubble. In section 2 we define the parameters for a numerical simulation, the initial geometry and show an example. In section 3, we discuss the numerical convergence criteria for our numerical simulation. We obtain very good numerical convergence with the mesh size for the first drop size and velocity, and discuss the variability observed for the subsequent droplets.

## 2 Numerical Method

We consider a bubble at rest at an air-water interface. The Young-Laplace equations fully describe the bubble shape, and its solution describes the profiles well observed experimentally for a bubble on an air-liquid interface [2, 4]. This problem involves two fluids separated by an interface. We note  $\rho_i$  and  $\mu_i$  the density and the viscosity of the fluid  $i$ ,  $\gamma$  the surface tension between the two fluids and  $g$  the gravity. Last, we note  $R_b$  the bubble radius which defines the characteristic length scale of the simulation. We can describe the problem by four dimensionless numbers, the viscosity ratio as  $\mu_{\text{liq}}/\mu_{\text{gaz}} = 55$ , the density ratio  $\rho_{\text{liq}}/\rho_{\text{gaz}} = 998$  which are close to the water-air condition, and the Laplace  $La$  and Bond  $Bo$  numbers,

$$La = \frac{\rho_{\text{liq}}\gamma R_b}{\mu_{\text{liq}}^2} \quad (1)$$

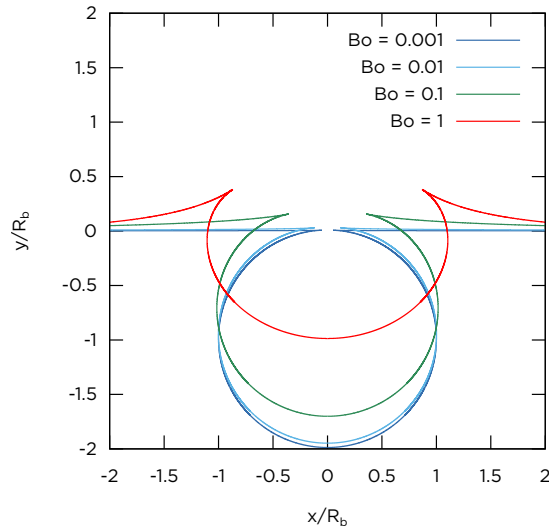


FIGURE 1 – Resolution of the Young-Laplace equation for 4 different Bond numbers. The length axes are rescaled by the characteristic length,  $R_b$ .

$$\text{Bo} = \frac{\rho_{\text{liq}} g R_b^2}{\gamma} \quad (2)$$

The Laplace number compares the capillary forces with the viscous forces. The Bond number compares the gravity forces with the capillary forces. The collapsing cavity generates a jet moving at velocity  $V$ , and we define the capillary number

$$\text{Ca} = \frac{V \mu_{\text{liq}}}{\gamma} \quad (3)$$

which compares the jet (or droplets) velocity with the visco-capillary velocity  $\gamma/\mu_{\text{liq}}$ . We normalize the droplets radii by the bubble radius  $r_d = R_d/R_b$ . Last, the timescale is made dimensionless by the use of the capillary timescale  $t_c = \sqrt{\rho_{\text{liq}} R_b^3/\gamma}$ .

Figure 1 shows the shape of the bubble for four different Bond numbers obtained by solving the Young-Laplace equation. The Laplace number does not impact the initial shape, which is determined by the balance between gravity and surface tension. In the no-gravity approximation, the bubble shape is a sphere. As we increase the Bond number, the shape differs more and more from the sphere. Increasing the gravity brings the bubble above the free surface, with a larger cavity, and smaller depth.

We perform 2D-axisymmetric simulations, using the Basilisk open-source library, to solve the incompressible two-phase Navier-Stokes equations with surface tension. We use an adaptive volume-of-fluid quad-tree mesh, which allows us to work up to an equivalent grid of a total of  $4^{14}$  points for a limited computation time. This library, based on the Gerris solver [15, 16], has been validated for different cases like breaking waves in 2D or in 3D [17, 18, 19, 20], atomizing jet [18, 21] or splashing [22, 23]. Since we work, with an adaptive mesh, a level 12 of maximum refinement means that we allow the mesh to refine itself up to  $2^{12}$  cells in each direction for a total of  $4^{12}$  cells, which gives us up to 820 cells along a bubble diameter.

We initialize the simulation with a bubble shape profile, as the one in the figure 1, at rest and without its top spherical cap, following [10, 24]. Figure 2 shows the time evolution of a bursting bubble for  $\text{Bo} = 0.1$  and  $\text{La} = 20000$ . It starts with the initial shape on the top left panel. We set the maximum refinement level

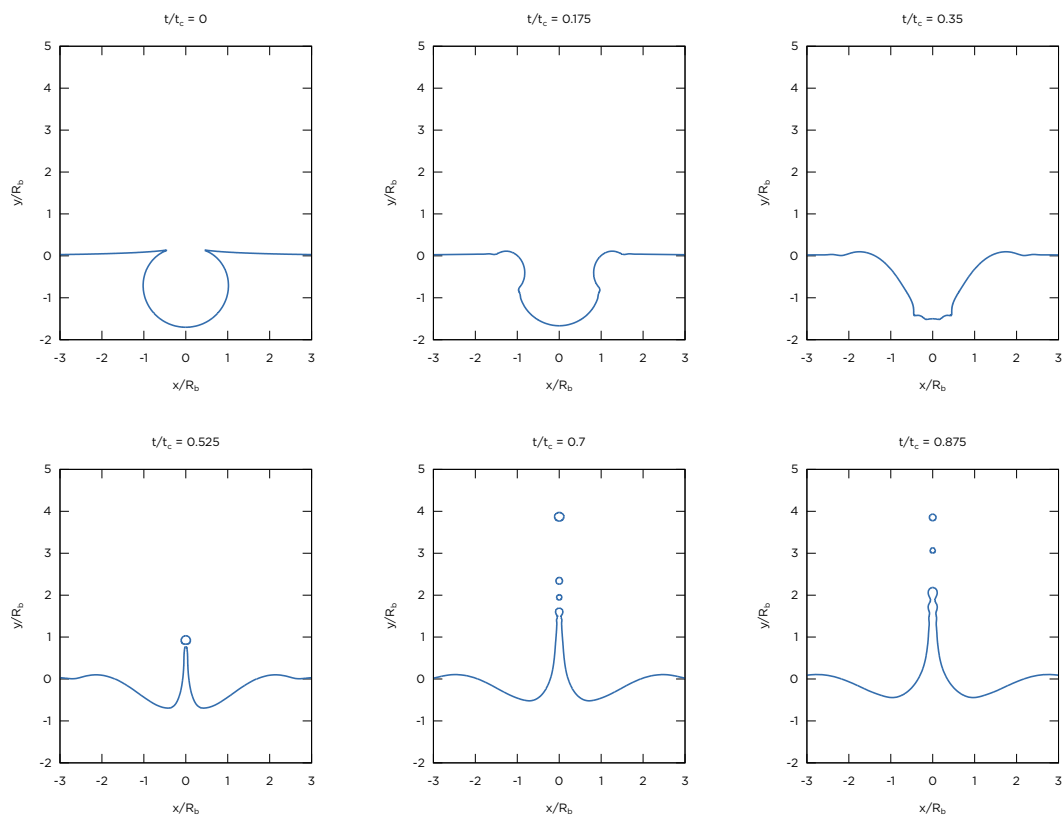


FIGURE 2 – Time evolution of a bursting bubble. The Bond number is set to 0.1 and the Laplace number is set to 20000. The mesh maximum refinement level is set to 12. The top panel of the figure shows the cavity collapse. The bottom panels show the rise of the jet and the formation of some droplets.

at 12. We plot the interface for  $t/t_c = 0, 0.175, 0.35, 0.525, 0.7, 0.875$ . The bubble cavity is collapsing due to the surface tension [4, 24] with waves propagating towards the center as described in [4, 10]. Then a jet forms at the center of the cavity. This jet rises up and breaks up to produce typically from 1 to 10 droplets depending on the control parameters.

### 3 Numerical Convergence of the Simulations

Here, we perform a convergence study of our numerical simulations, by changing the maximum level of refinement. We choose to start at level 12 and to increase it up to level 14 for one specific case. This method can be extended to all the possible Bond and Laplace numbers. For this case, we consider the Bond number  $Bo = 0.1$  and the Laplace number  $La = 20000$ . The code adapts the mesh with 2 criteria based on the error on the interface and on the velocity. The adaptive criteria for the mesh remain the same for the 3 refinement levels.

To estimate the numerical convergence of a simulation, we consider several output variables of the bursting process. We know from previous numerical and experimental studies that the first drop behavior is well defined [4, 6, 8, 10]. Therefore, we start by analyzing the interface profile of the jet for different times, the position of the top of the jet during the entire simulation, the velocity of the top of the jet, the ejection velocity of the droplets and the size of the droplets.

Figure 3 shows the superposition of 3 interface profiles for 6 different time steps, at  $t/t_c$  is 0.35, 0.4, 0.45, 0.5, 0.55 and 0.6, represented in the panel (a), (b), (c), (d), (e) and (f). On panel (a), the profiles are almost on top of each other. On panel (b), we see only very small differences between the profiles at the bottom of the cavity. The jet starts forming on this panel, and the differences are small, when we take into account the velocities of the jets at that point (see figure 4). On panel (c), the jets start to rise. The profiles for levels 13 and 14 are almost on top of each other. There is a very small difference with the profile at level 12. On the last 3 panels ((d) to (f)), we see bigger differences, around the top of each jet. The drops detach from the jets at different times. However, we show that the velocity and the radius of the first drop are numerically converged (see figure 6). As the jets continue to rise, we see small differences at their tops where new drops form.

Figure 4 shows the time evolution of the velocity of the top of the jet. The curves are almost on top of each other up to a time close to  $t/t_c \approx 0.5$ . At that point, the jet velocity at level 14 decays suddenly. This corresponds to the ejection of a droplet. The same thing occurs for levels 13 and 12. The decay is the same and the 3 jet reaches the same new velocity. The droplet production occurs at different times. Even if the droplets production occurs at different times, the velocities of the jets are the same for the 3 levels before and after the droplets production (characterize by the sudden decay of each velocity). Thus, we are confident that the jet dynamic is numerically converged for this case.

Figure 5 shows the time evolution of the top of each jet and the center of mass of each droplet during the simulations, for the 3 levels of refinement. We recover our observations from the figure 3 : the jet behavior is the same up to  $t/t_c = 0.6$ . After that time, the droplets production occurs for very different times. From  $t/t_c = 0.6$  to 0.8, the level 12 produces 2 droplets on the same time which merge a few steps later, the levels 13 and 14 produce 2 droplets at 2 different times with 2 different behaviors. We consider that the droplets 2 and 3 for the level 12 are the same, since they merge very quickly after their production. At the end of the simulation, the level 14 is ejecting a fourth drop before going down. This is not the case for the 2 other levels.

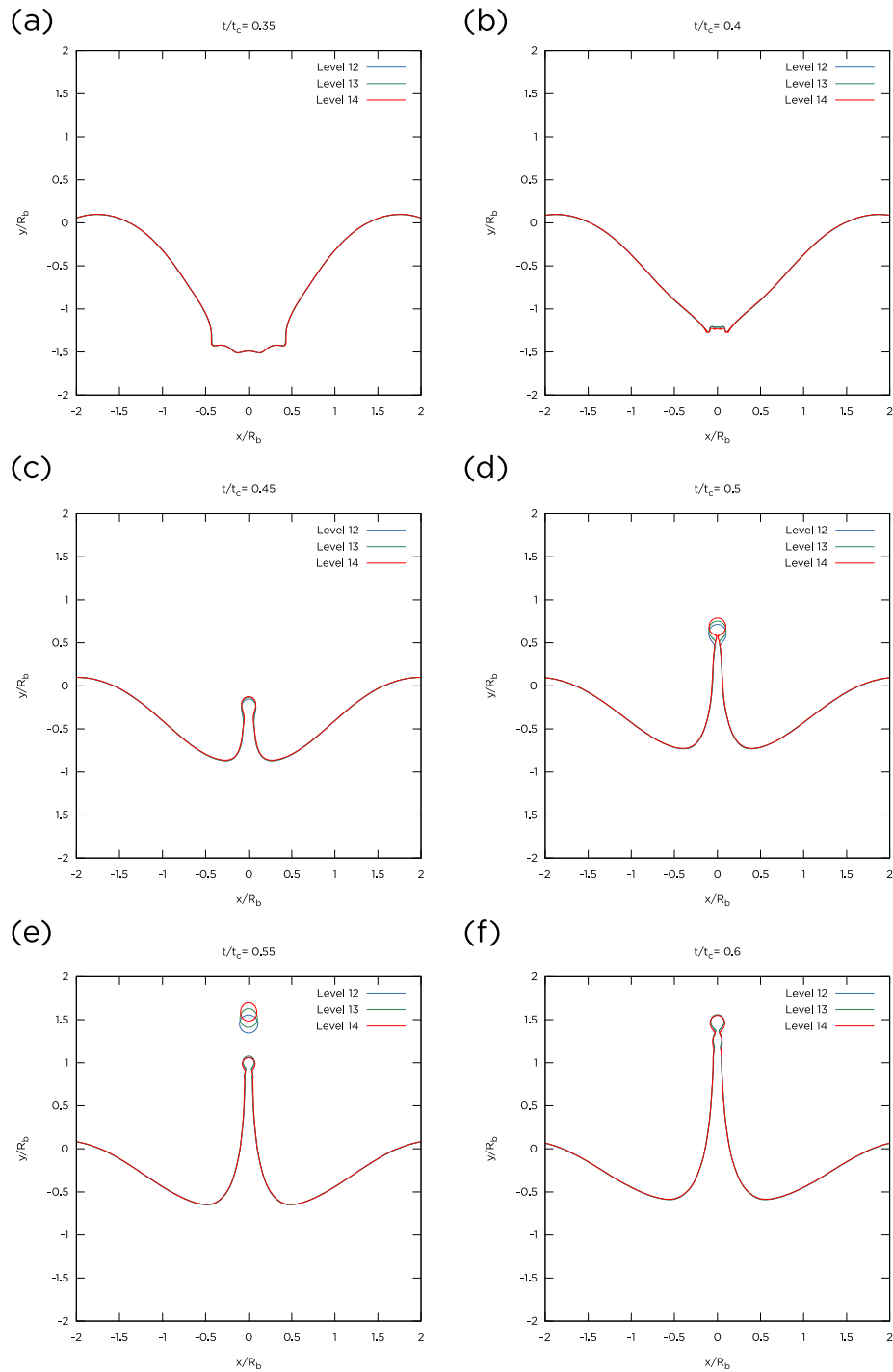


FIGURE 3 – We compare the interface of the simulations for 6 different time steps, for 3 levels of refinement, from 12 to 14. (a) shows that the profiles for the 3 different resolutions are superposed at  $t/t_c = 0.35$ . The 3 interface profiles are very close to each other. (b) shows the interface profiles at the beginning of the formation of the jet at  $t/t_c = 0.4$ . We observe only small differences between the level 14 and the other 2 levels. (c) shows the interfaces for  $t/t_c = 0.45$ . The jet is now formed and starts to rise. There is a good agreement between the levels 14 and 13. The end of the jet is a bit thicker and has risen a bit less for the level 12. (d) shows the end of the pinching process. The drop detaches almost from the jet for the level 14, whereas it is still in formation for levels 13 and 12. (e) shows the profile after the production of the first drop. The drop profiles are more different than at earlier time, while the jet profiles are still very close. (f) shows the jets profiles for  $t/t_c = 0.6$ , with small differences between the level 14 and the 2 lower levels.

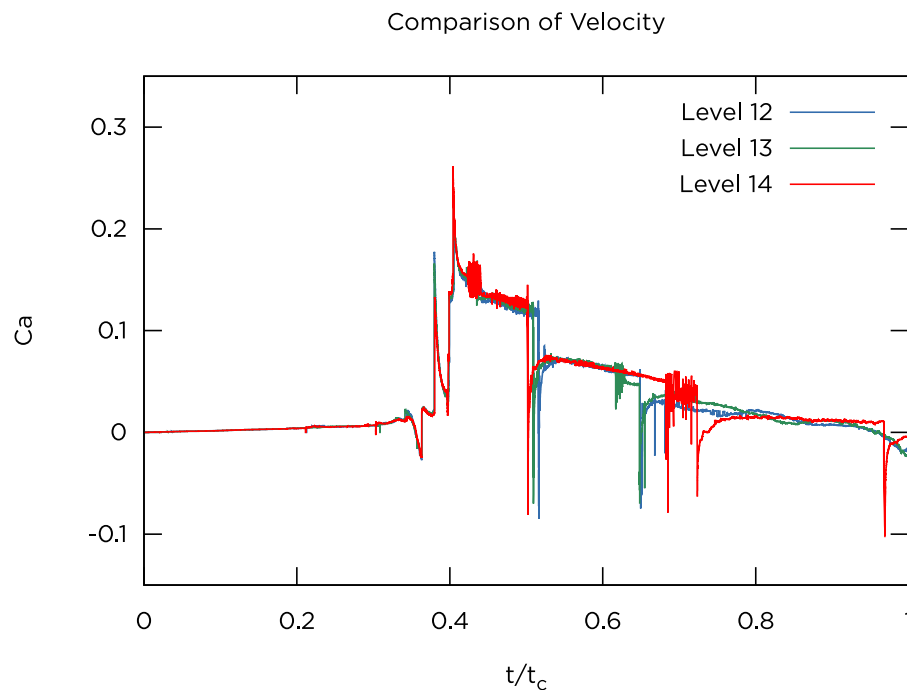


FIGURE 4 – Capillary velocity  $Ca$  of the top point of the jet for 3 different meshes as a function of time  $t/t_c$ . Up to  $t/t_c < 0.45$ , the velocity is globally the same for the three resolutions. At  $t/t_c \sim 0.45$ , we see a sharp decay in the jet velocity, due to the formation of one drop. The jet detachment occurs at different times for the 3 meshes. This was also observed in [10]. After the first drop, the general behaviors are similar, but not the breakup times (corresponding to the sudden decay in the jet velocity).

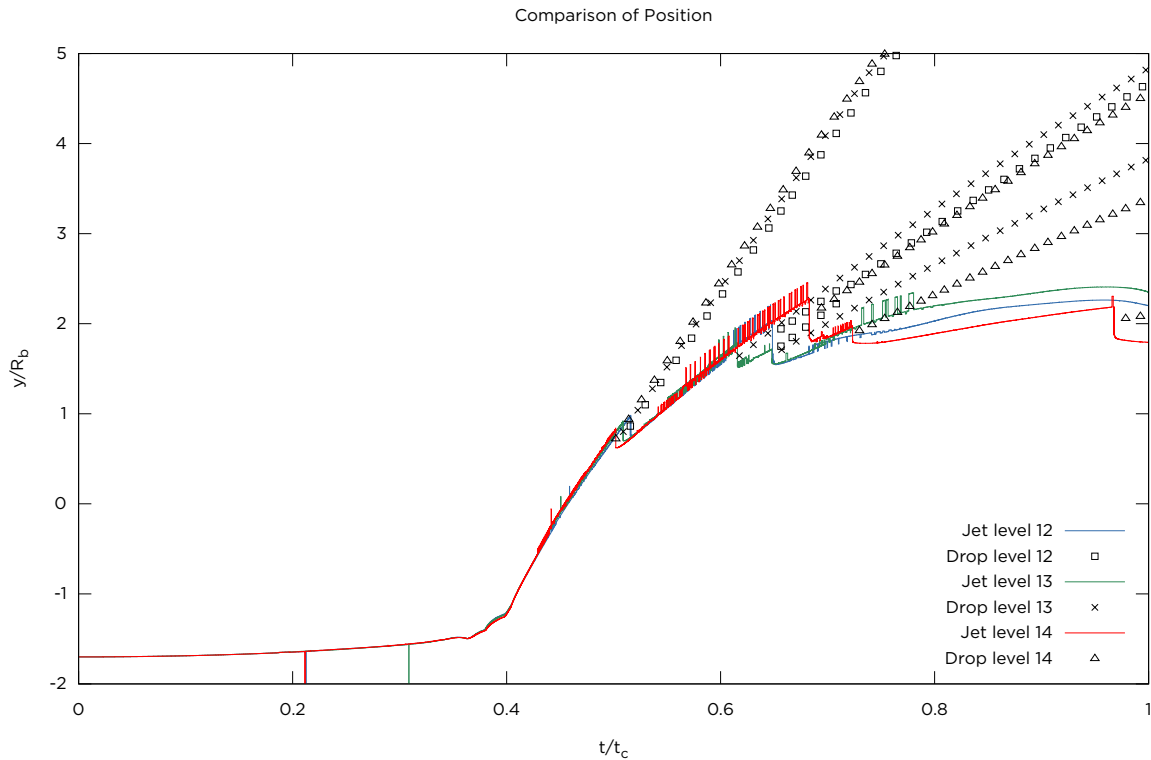


FIGURE 5 – Position of the top of the jet and the center of mass of the ejected droplet for 3 different meshes, as a function of time  $t/t_c$ . The squares represent the drop for the level 12, the crosses are for the level 13 and the triangles for the level 14. The jet positions are the same up to the ejection of the first drop. The ejection occurs at slightly different times. However, the trajectory of the first drop is the same for the 3 meshes. Then, up to  $t/t_c = 0.6$ , the trajectories of the jets at different resolutions are the same again. Then, the 3 jets at different mesh resolutions eject droplets at slightly different times, with variation in sizes. However, the top of the jet behaves the same way for each mesh.

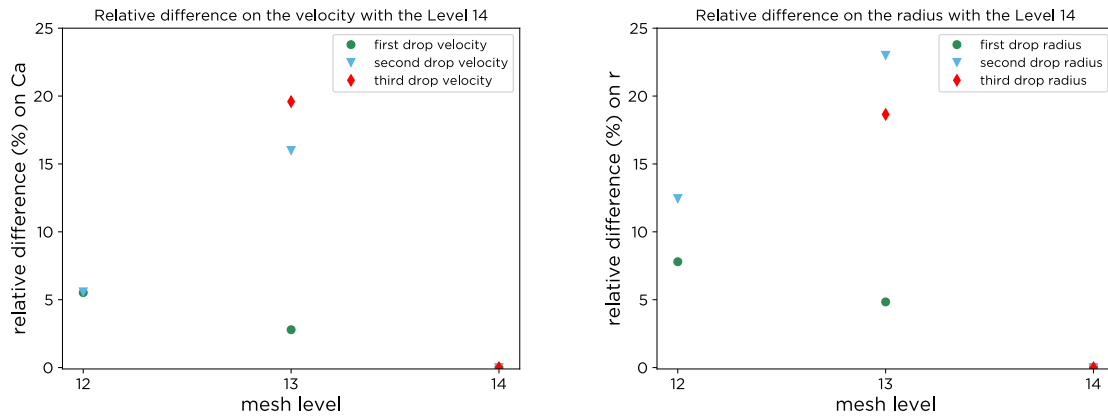


FIGURE 6 – We compare the results of the first 3 drops for 3 meshes. The level 14 is chosen as the reference level and we show the error of the velocity and the droplet size with respect to the highest resolution. The left panel represents the error on the capillary velocity  $Ca$  as a function of the mesh and the right panel stands for the first three droplets radius errors as a function of the mesh size. As we increase the level, we decrease the differences with the mesh at level 14 for the first drop. With less than 5% of difference between the level 13 and 14, the simulation is numerically converged. For the 2 other droplets (numbers 2 and 3), larger differences are visible, showing the sensitivity of the droplet size and velocity to the details of the numerical resolution.

Figure 6 compares the velocities and the sizes of the droplets for the simulations at levels 12 and 13 with the one at level 14. The level 13 is close to the level 14 for the first drop, with less than 5% of difference on the size, and less than 2.5% of difference on the velocity. This is small enough to say that the simulations are numerically converged for the first drop. However, the second and the third drop are much different for each level (up to 23% of difference). Experiments show that the characteristics of the drops coming after the first one present some large variations from one experiment to the other [5, 25]. The study of the droplets coming after the first one has to be done statistically if we want to have a good comprehension of their behavior.

Through this example, we show that the dynamic of the jet and the breakup process are numerically converged up to the first drop. After the first drop, we have to be careful on the results. One simulation can only give us a general trend and not the full behavior of the jet. A statistical study has to be done to obtain the general behavior of the jet after the first drop.

## 4 Conclusion

In this article we present a highly resolved numerical simulation able to reproduce the jetting process associated with the bursting of a bubble. We discuss and define numerical convergence criteria for the simulation. We apply those criteria on a specific case as an example. We can extend this work to a broad range of Laplace and Bond number. Once the numerical convergence is achieved, these simulations can be compared with experimental, numerical and theoretical results from the literature. From these simulations, we can extract the dynamics of all the droplets produced by bubble bursting. We remark that while numerical convergence is achieved to a great accuracy for the first drop size and velocity, the subsequent drops present large variability in their dynamics, showing high sensitivity to the initial condition posed by the first drop detachment. Therefore, a statistical study has to be done for the droplets after the first one to give a full picture of the jet drop formation.

This material is based upon work supported by the National Science Foundation under Grant No. 1849762. L.D. thanks the Cooperative Institute for Earth System modeling between Princeton and GFDL NOAA, and the International Fund from Princeton University.

## Références

- [1] Fabrice Veron. Ocean Spray. *Annual Review of Fluid Mechanics*, 47(1) :507–538, January 2015.
- [2] H. Lhuissier and E. Villermaux. Bursting bubble aerosols. *Journal of Fluid Mechanics*, 696 :5–44, April 2012.
- [3] Laurent Duchemin, Stéphane Popinet, Christophe Josserand, and Stéphane Zaleski. Jet formation in bubbles bursting at a free surface. *Physics of Fluids*, 14(9) :3000–3008, September 2002.
- [4] Elisabeth Ghabache, Arnaud Antkowiak, Christophe Josserand, and Thomas Séon. On the physics of fizziness : How bubble bursting controls droplets ejection. *Physics of Fluids*, 26(12) :121701, December 2014.
- [5] Donald E. Spiel. The number and size of jet drops produced by air bubbles bursting on a fresh water surface. *Journal of Geophysical Research*, 99(C5) :10289, 1994.
- [6] Elisabeth Ghabache and Thomas Séon. Size of the top jet drop produced by bubble bursting. *Physical Review Fluids*, 1(5), September 2016.
- [7] Gérard Liger-Belair, Guillaume Polidori, and Philippe Jeandet. Recent advances in the science of champagne bubbles. *Chemical Society Reviews*, 37(11) :2490, 2008.
- [8] Elisabeth Ghabache, Gérard Liger-Belair, Arnaud Antkowiak, and Thomas Séon. Evaporation of droplets in a Champagne wine aerosol. *Scientific Reports*, 6(1), July 2016.
- [9] A. H. Woodcock, C. F. Kientzler, A. B. Arons, and D. C. Blanchard. Giant Condensation Nuclei from Bursting Bubbles. *Nature*, 172(4390) :1144–1145, December 1953.
- [10] Luc Deike, Elisabeth Ghabache, Gérard Liger-Belair, Arup K. Das, Stéphane Zaleski, Stéphane Popinet, and Thomas Séon. Dynamics of jets produced by bursting bubbles. *Physical Review Fluids*, 3(1), January 2018.
- [11] C. Frederik Brasz, Casey T. Bartlett, Peter L. L. Walls, Elena G. Flynn, Yingxian Estella Yu, and James C. Bird. Minimum size for the top jet drop from a bursting bubble. *Physical Review Fluids*, 3(7), July 2018.
- [12] Alfonso M. Gañán-Calvo. Revision of Bubble Bursting : Universal Scaling Laws of Top Jet Drop Size and Speed. *Physical Review Letters*, 119(20), November 2017.
- [13] Alfonso M. Gañán-Calvo. Scaling laws of top jet drop size and speed from bubble bursting including gravity and inviscid limit. *Physical Review Fluids*, 3(9), September 2018.
- [14] J. M. Gordillo and J. Rodríguez-Rodríguez. Capillary waves control the ejection of bubble bursting jets. *Journal of Fluid Mechanics*, 867 :556–571, May 2019.
- [15] Stéphane Popinet. An accurate adaptive solver for surface-tension-driven interfacial flows. *Journal of Computational Physics*, 228(16) :5838–5866, September 2009.
- [16] Stéphane Popinet. Numerical Models of Surface Tension. *Annual Review of Fluid Mechanics*, 50(1) :49–75, January 2018.
- [17] Luc Deike, W. Kendall Melville, and Stéphane Popinet. Air entrainment and bubble statistics in breaking waves. *Journal of Fluid Mechanics*, 801 :91–129, August 2016.

- [18] Daniel Fuster, Gilou Agbaglah, Christophe Josserand, Stéphane Popinet, and Stéphane Zaleski. Numerical simulation of droplets, bubbles and waves : State of the art. *Fluid Dynamics Research*, 41(6) :065001, December 2009.
- [19] Luc Deike, Stephane Popinet, and W. Kendall Melville. Capillary effects on wave breaking. *Journal of Fluid Mechanics*, 769 :541–569, April 2015.
- [20] Luc Deike, Luc Lenain, and W. Kendall Melville. Air entrainment by breaking waves. *Geophysical Research Letters*, 44(8) :3779–3787, April 2017.
- [21] Xiaodong Chen, Dongjun Ma, Vigor Yang, and Stephane Popinet. High-Fidelity Simulation of Impacting Jet Atomization. *Atomization and Sprays*, 23(12) :1079–1101, 2013.
- [22] Marie-Jean Thoraval, Kohsei Takehara, Takeharu Goji Etoh, Stéphane Popinet, Pascal Ray, Christophe Josserand, Stéphane Zaleski, and Sigurdur T. Thoroddsen. Von Kármán Vortex Street within an Impacting Drop. *Physical Review Letters*, 108(26), June 2012.
- [23] G. Agbaglah and R. D. Deegan. Growth and instability of the liquid rim in the crown splash regime. *Journal of Fluid Mechanics*, 752 :485–496, August 2014.
- [24] Ching-Yao Lai, Jens Eggers, and Luc Deike. Bubble Bursting : Universal Cavity and Jet Profiles. *Physical Review Letters*, 121(14), October 2018.
- [25] Elisabeth Ghabache. *Surface Libre Hors Équilibre : De l’effondrement de Cavité Aux Jets Étirés*. PhD thesis.